

SANDIA REPORT

SAND2017-0957
Unlimited Release
March 2017

Performance Comparison of Stion CIGS Modules to Baseline Monocrystalline Modules at the New Mexico, Florida, and Vermont Regional Test Centers: January 2015-December 2016

Matthew Lave, Joshua S. Stein, Laurie Burnham

Prepared by
Sandia National Laboratories
Albuquerque, New Mexico 87185 and Livermore, California 94550

Sandia National Laboratories is a multi-mission laboratory managed and operated by Sandia Corporation, a wholly owned subsidiary of Lockheed Martin Corporation, for the U.S. Department of Energy's National Nuclear Security Administration under contract DE-AC04-94AL85000.

Approved for public release; further dissemination unlimited.



Issued by Sandia National Laboratories, operated for the United States Department of Energy by Sandia Corporation.

NOTICE: This report was prepared as an account of work sponsored by an agency of the United States Government. Neither the United States Government, nor any agency thereof, nor any of their employees, nor any of their contractors, subcontractors, or their employees, make any warranty, express or implied, or assume any legal liability or responsibility for the accuracy, completeness, or usefulness of any information, apparatus, product, or process disclosed, or represent that its use would not infringe privately owned rights. Reference herein to any specific commercial product, process, or service by trade name, trademark, manufacturer, or otherwise, does not necessarily constitute or imply its endorsement, recommendation, or favoring by the United States Government, any agency thereof, or any of their contractors or subcontractors. The views and opinions expressed herein do not necessarily state or reflect those of the United States Government, any agency thereof, or any of their contractors.

Printed in the United States of America. This report has been reproduced directly from the best available copy.

Available to DOE and DOE contractors from

U.S. Department of Energy
Office of Scientific and Technical Information
P.O. Box 62
Oak Ridge, TN 37831

Telephone: (865) 576-8401
Facsimile: (865) 576-5728
E-Mail: reports@osti.gov
Online ordering: <http://www.osti.gov/scitech>

Available to the public from

U.S. Department of Commerce
National Technical Information Service
5301 Shawnee Rd
Alexandria, VA 22312

Telephone: (800) 553-6847
Facsimile: (703) 605-6900
E-Mail: orders@ntis.gov
Online order: <http://www.ntis.gov/search>



SAND2017-0957
March 2017

**Performance Comparison of Stion CIGS Modules
to Baseline Monocrystalline Modules at the New Mexico,
Florida, and Vermont Regional Test Centers:
January 2015-December 2016**

Matthew Lave
Photovoltaic and Distributed Systems Integration
Sandia National Laboratories
P.O. Box 969, MS-9052
Livermore, CA 94551-0969

Joshua S. Stein
Photovoltaics and Distributed Systems Integration
Sandia National Laboratories
P.O. Box 5800
Albuquerque, New Mexico 87185-MS1033

Laurie Burnham
Electric Power Systems Research
Sandia National Laboratories
P.O. Box 5800
Albuquerque, New Mexico 87185-MS1140

ABSTRACT

This report provides performance data and analysis for two Stion copper indium gallium selenide (CIGS) module types, one framed, the other frameless, and installed at the New Mexico, Florida and Vermont RTCs. Sandia looked at data from both module types and compared the latter with data from an adjacent monocrystalline baseline array at each RTC. The results indicate that the strings produce slightly more than their rated power output at conditions near standard test conditions, as indicated by DC performance ratios slightly above 1 at irradiances near 1000Wm^{-2} and cell temperatures near 25°C . In addition, Sandia sees no significant performance differences between the two Stion module types, which is expected because the modules differ only in their framing. In contrast to the baseline systems, the Stion strings showed increasing DC performance ratios with increasing irradiance, with the greatest increase between zero and 400Wm^{-2} but still noticeable increases at 1000Wm^{-2} . Although baseline data availability in Vermont was spotty and therefore comparative trends are difficult to discern, the Stion modules there may offer snow-shedding advantages over monocrystalline-silicon modules but these findings are preliminary.

CONTENTS

1.	Introduction	9
2.	Data	10
2.1	System Descriptions.....	10
2.2	Data Monitoring and Measurements.....	11
2.3	Data Availability.....	12
2.4	Quality Control	12
2.4.1.	Solar-Time Filter.....	12
2.4.2.	Current-Irradiance Filter	13
3.	Results	16
3.1.	Weather Differences at the RTCs	16
3.2.	Cell Temperatures	18
3.3.	Impact of Snow Cover	19
3.4.	DC Performance Ratio	21
3.4.1.	Performance Ratio at Constant Irradiance	21
3.4.2.	Performance Ratio at Constant Temperature	22
3.4.3.	DC Performance Ratio Joint Dependence on Irradiance and Temperature	24
3.4.4.	Monthly DC Performance Ratio	25
4.	Conclusions	28

FIGURES

Figure 1: Photo of the meteorological instrumentation	11
Figure 2: Data availability	12
Figure 3: Baseline reference cell irradiance (colors)	13
Figure 4: Reference cell irradiance in New Mexico on a clear day in December	13
Figure 5: Current-irradiance data from the New Mexico RTC.....	14
Figure 6: Current and irradiance date for a 12-hour period with filtered data indicated	14
Figure 7: Current [top plot] and reference cell irradiance [bottom plot] for baseline string 1	15
Figure 8: Two-dimensional histograms	17
Figure 9: Cell temperatures.....	18
Figure 10: Stion versus baseline cell temperatures.....	19
Figure 11: Impact of snow at Vermont RTC	20
Figure 12: Photo (left) showing the contrast in snow cover	20
Figure 13: Relative DC performance ratio (y-axis) as a function of cell temperature	22
Figure 14: DC performance ratio (y-axis) as a function of reference cell irradiance	22
Figure 15: Top Plots: Voltage and current, temperature corrected and normalized by manufacturer data sheet values, plotted as a function of irradiance. Bottom plots: temperature corrected PRDCas a function of irradiance. Left side plots shows baseline array two and right side plots show the aggregate of Stion arrays 1-4.....	23
Figure 16: Maximum power point voltage, as measured from a module mounted on a tracker,, temperature corrected and normalized by spec sheet value, plotted as a function of irradiance for (left) a baseline module and (right) a Stion module. The axis range is the same as the top plots of Figure 15 to allow for comparison.....	24
Figure 17: DC performance ratio (colors) as a function of reference-cell irradiance.....	25
Figure 18: Monthly PRDCin New Mexico.....	26
Figure 19: Monthly PRDCin Florida.....	27
Figure 20: Monthly PRDCin Vermont	27

TABLES

Table 1: Systems Considered	10
Table 2: Data-Monitoring System for the Stion and Baseline Arrays	11

1. INTRODUCTION

In 2014, Stion, a US manufacturer of thin-film copper gallium indium selenide (CIGS) modules, applied to the US Department of Energy's Regional Test Center (RTC) Program for Solar Technologies¹ requesting a performance validation of its modules at the New Mexico, Florida and Vermont RTCs. This report provides data and analysis for a 12kW Stion system, divided equally into subarrays of framed and frameless CIGS modules, at all three sites, and also compares the DC performance ratio of the Stion PV system with a 6kW monocrystalline silicon (C-Si) reference PV system at each site.

An important aim of this study is to demonstrate and quantify the field performance of Stion modules in climates representing a range of irradiance, temperature and moisture conditions and to compare the overall reliability and performance of the Stion arrays with the RTC baseline array. A secondary aim of the study is to improve our basic understanding of the reliability and performance of CIGS technologies. Although CIGS has less than 5% of the solar-cell market today, the thin-film technology is expected to see its market share increase as cell efficiencies increase, thus rendering CIGS modules cost competitive with silicon modules. In addition, assessing the performance of Stion's glass/glass module technology in high-humidity climates is of interest because industry projections call for a growth in glass/glass modules from 3% in 2015 to an expected 20% by 2026.²

¹ For more information on the RTC program: <https://rtc.sandia.gov>

² International Technology Roadmap for Photovoltaic, Seventh Edition, March 2016

2. DATA

2.1 System Descriptions

The two systems considered in this analysis are the RTC reference, or baseline, system, which is comprised of 6kW of monocrystalline PV modules and a 12kW Stion system, which has two subarrays, one populated with CIGS frameless glass/glass modules (Stion STL-140A); the other with an identical set of Stion modules but the latter are framed (Stion STO-140A.) [See Table 1 for more system details.] The systems in NM and VT are at a 35° latitude; the FL system is at a 30° tilt. All systems face south.

Table 1: Systems Considered

PV System	Module Type	Module Pmax	Arrays	Strings	Modules per String	Inverter Type	Total kW
Baseline _{NM}	Suniva OPT 270-60-4	270W	1	2	12	Fronius IG Plus Advanced 3.0-1-UNI	6.48kW
						SMA Sunny Boy 3800-US	
Stion _{NM}	Stion STL- 140A (array 1)	140W	2	4	11	SMA 15000TL- US	12.32kW
	Stion STO- 140A (array 2)						
Baseline _{FL}	Suniva OPT 270-60-4	270W	1	2	12	Fronius IG Plus Advanced 3.0-1-UNI	6.48kW
						SMA Sunny Boy 3800-US	
Stion _{FL}	Stion STL- 140A (array 1)	140W	2	4	11	SMA 15000TL- US	12.32kW
	Stion STO- 140A (array 2)						
Baseline _{VT}	Suniva OPT 270-60-4	270W	1	2	12	Fronius IG Plus Advanced 3.0-1-UNI	6.48kW
						SMA Sunny Boy 3800-US	
Stion _{VT}	Stion STL- 140A (array 1)	140W	2	4	11	SMA 15000TL- US	12.32kW
	Stion STO- 140A (array 2)						

2.2 Data Monitoring and Measurements

The RTC high-resolution data-monitoring system collects data at no less than five-second-intervals and averages the data at one-minute intervals (see Table 2.) Data collected includes DC voltage and current at the string level (multiplied together to calculate total DC power); module temperature (measured by thermocouples on multiple modules); and plane-of-array (POA) irradiance sensors, one of which is cleaned twice a week; the other left to soil naturally. For this analysis, we have relied on data from the cleaned cell

Table 2: Data-Monitoring System for the Stion and Baseline Arrays

Performance Measurement	Sensor Type
Irradiance	Kipp & Zonen CMP-11
PV Reference Cell	EETS cell
Temperature	Omega Type-T thermocouples
DC voltage	Resistive voltage divider with accuracy of 0.1%.
DC current	Empro current shunts with accuracy of 0.1%



Figure 1: Photo of the meteorological instrumentation mounted on the west end of the Stion STO-140 array. Ambient temperature is measured by a shielded thermocouple (upper left); irradiance levels are measured by a plane-of-array pyranometer and two EETS reference cells, one of which is cleaned twice a week; the other is left to soil naturally.

2.3. Data Availability

This report includes available data from a nearly two year period (from January 1, 2015 through December 8, 2016) but the availability of data during that period varies, reflecting 1) different commissioning dates for the two systems (baseline and Stion) at the three RTC sites, and 2) outages at both the New Mexico and Vermont sites (see Figure 2).

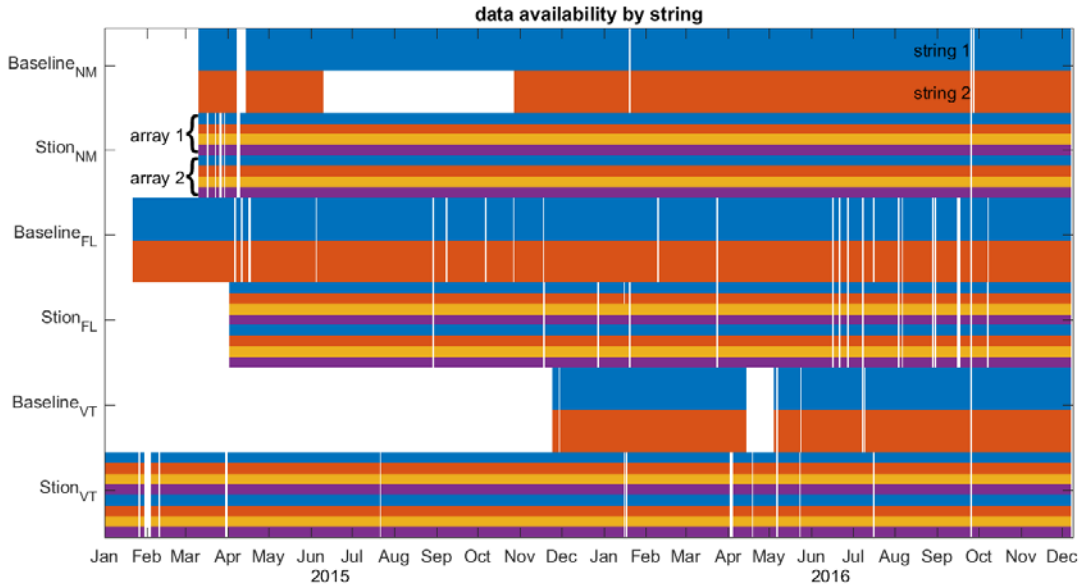


Figure 2: Data availability for the New Mexico, Florida and Vermont VT RTCs. As depicted above, the baseline system (string 2) in NM had a significant outage in summer 2015; the VT baseline system did become fully functional until December 2015; and a data outage affected the VT baseline in May 2016.

2.4. Quality Control

2.4.1. Solar-Time Filter

For the purposes of this report, Sandia filtered the data to only include measurements from 4 hours before and after solar noon, as shown in Figure 3. We applied this filter to all sites to eliminate (a) nighttime and small irradiance values, and (b) uneven early morning and late afternoon shading at the New Mexico RTC created in the east field-of-view (mountains) and the west field-of-view (buildings).

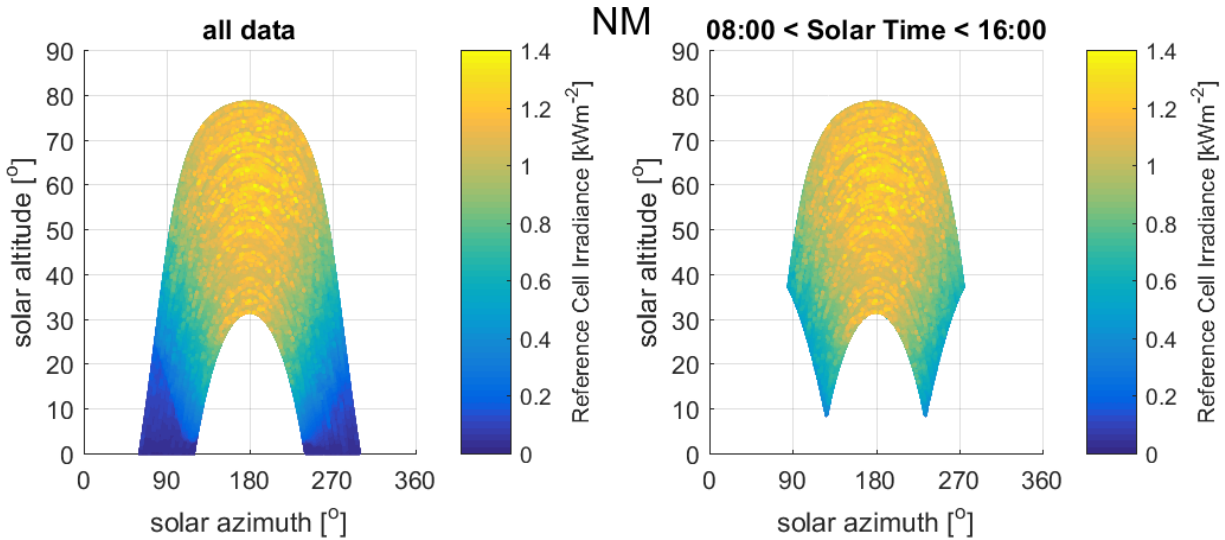


Figure 3: Baseline reference cell irradiance (colors) plotted as a function of solar azimuth and solar altitude (New Mexico RTC data).

The impact of the solar-time filter is seen in Figure 4, which depicts data from the New Mexico RTC, with eliminated (i.e., filtered) times highlighted in red. A sharp increase in irradiance is seen around 7:30 solar time, as the sun clears the mountain horizon to the east. In the evening, a decrease in irradiance is seen around 16:30, but it is more gradual and occurs slightly later. Scattered buildings to the west of the modules are likely responsible for this shading pattern. The solar-time filter removes both of these shaded periods from the analysis. The filter is applied symmetrically (though a filter just to remove the evening shading might be suitable) to ensure that both morning and evening performance are considered equally in the analysis that follows.

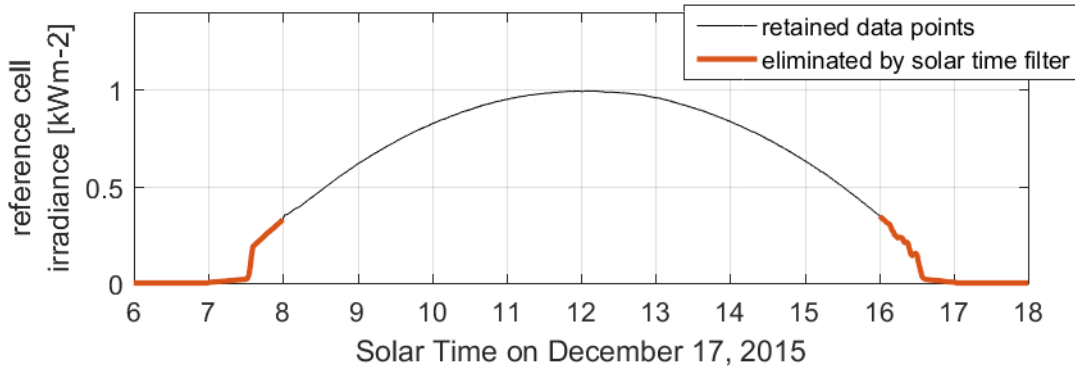


Figure 4: Reference cell irradiance in New Mexico on a clear day in December, with points eliminated by the solar time filter highlighted in red.

2.4.2. Current-Irradiance Filter

In addition to the solar-time filter, we applied a current-irradiance filter to all locations and all strings to capture the relationship between the current and the reference cell irradiance. This current-irradiance filter eliminated values for which the measured current deviated by more than 30% from the current that is predicted by the equation $I = I_{mpp,STC} \times Irr_{ref\ cell}$, where $I_{mpp,STC}$ is the STC maximum power point current (8.7A for the baseline system, 2.34A for the Stion

system) and $Irr_{ref\ cell}$ is the reference cell irradiance, expressed in kWm^{-2} . This result of the current-irradiance filter in New Mexico is shown in Figure 5.

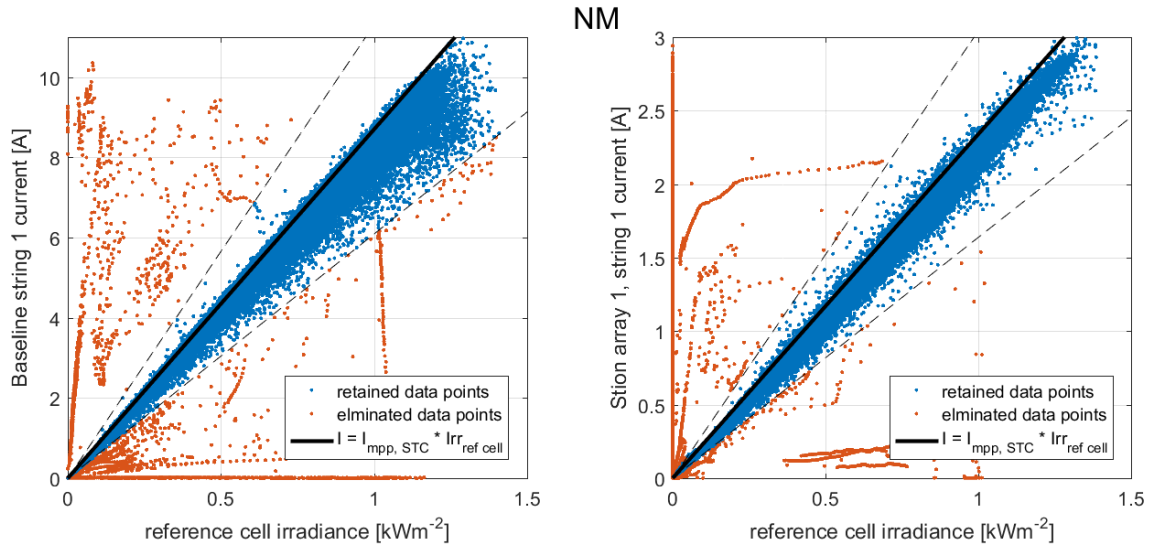


Figure 5: Current-irradiance data from the New Mexico RTC. The above graphs depict current as a function of reference-cell irradiance, with data points filtered out from the analysis (red dots). Baseline string 1 current (left), and Stion array 1, string 1 current (right).

We applied the current-irradiance filter to eliminate faulty current data, which manifests itself as measurement values that drop to nearly zero instantaneously. This effect can be seen in Figure 6 just after 14:00 when the current drops to near zero, even though the irradiance is nonzero.

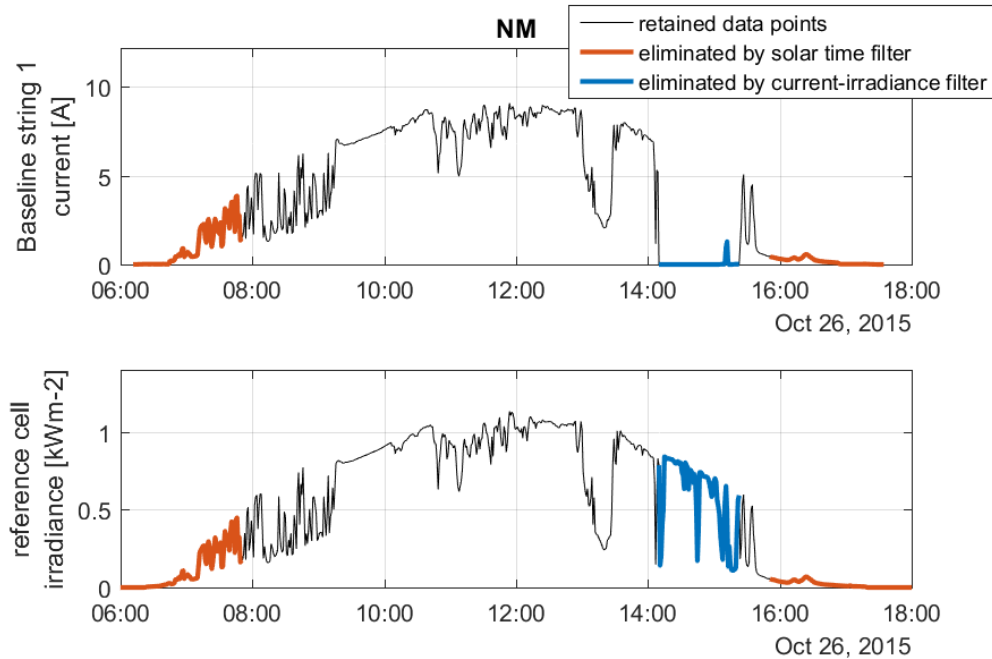


Figure 6: Current and irradiance data for a 12-hour period with filtered data indicated in blue and red. Current (top plot) and reference cell irradiance (bottom plot) for baseline string 1 on a day in New Mexico with errant current measurements. The errant measurements are filtered out by the current-irradiance filter (blue line) and also by the solar-time filter (red line).

A second benefit of the current-irradiance filter is that it removes data from days when snow accumulated on either the Stion modules or the baseline modules at a different rate than on the POA reference cell. For example, it snowed in Albuquerque on December 26th and 27th, 2015, and temperatures remained below freezing on December 28th, leading to slow snow melt. We see in Figure 7 that the snow appears to have impacted the baseline PV modules less (December 27th) and to have melted faster on the baseline modules (December 28th) than on the reference cell.

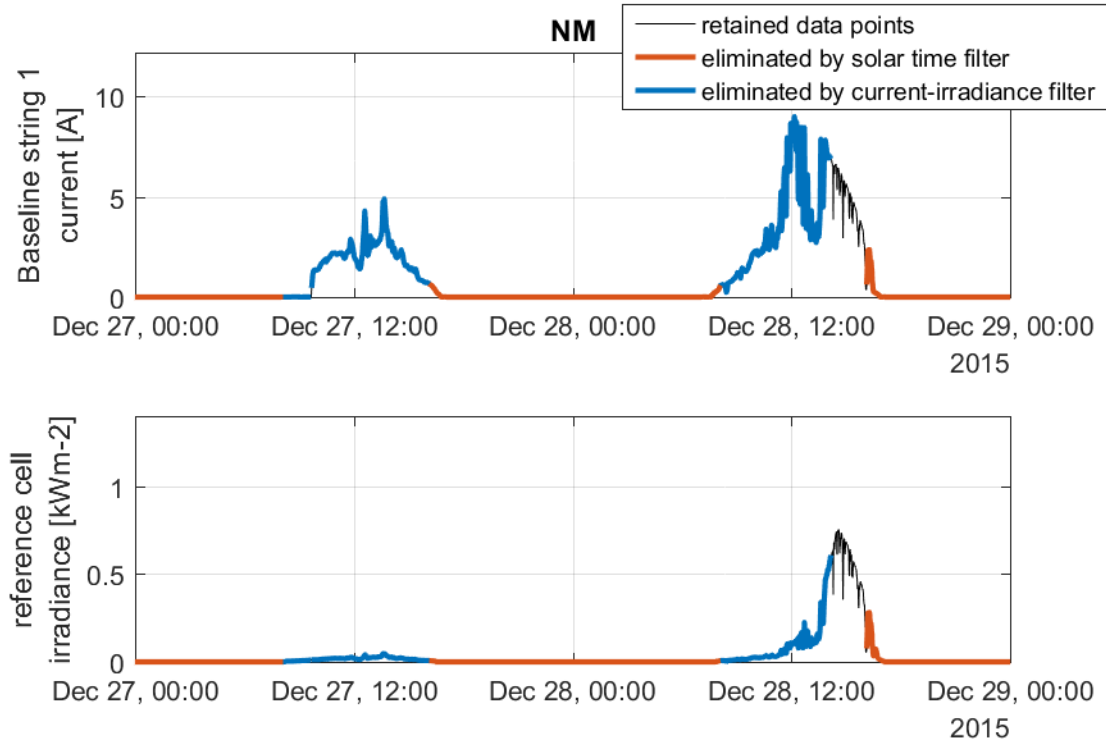


Figure 7: Current [top plot] and reference cell irradiance [bottom plot] for baseline string 1 on a day in New Mexico when snow was present and differentially affected the modules versus the reference cell.

3. RESULTS

3.1. Weather Differences at the RTCs

Each of the Stion systems was installed at climatically distinct site, with a distinct irradiance profile (see Figure 8 for the distribution of irradiance and ambient temperature at the three locations.) Because of solar-time filtering, high irradiances are common across all three sites but New Mexico skews toward large irradiances, reflecting often clear-sky conditions; Florida toward uniformity because of its partly cloudy weather where cloud intermittency introduces irradiance levels that alternate quickly between high and low; and Vermont toward a bimodal distribution, with separate peaks at high and low irradiances, indicating that Vermont skies are typically either fully clear or fully cloudy.

Ambient temperatures vary similarly. New Mexico temperatures are almost always in the 0°C to 40°C range. Florida temperatures vary less, but like New Mexico, are almost always between 10°C and 40°C. Vermont temperatures occupy a lower range: temperatures there are generally between -20°C and 30°C.

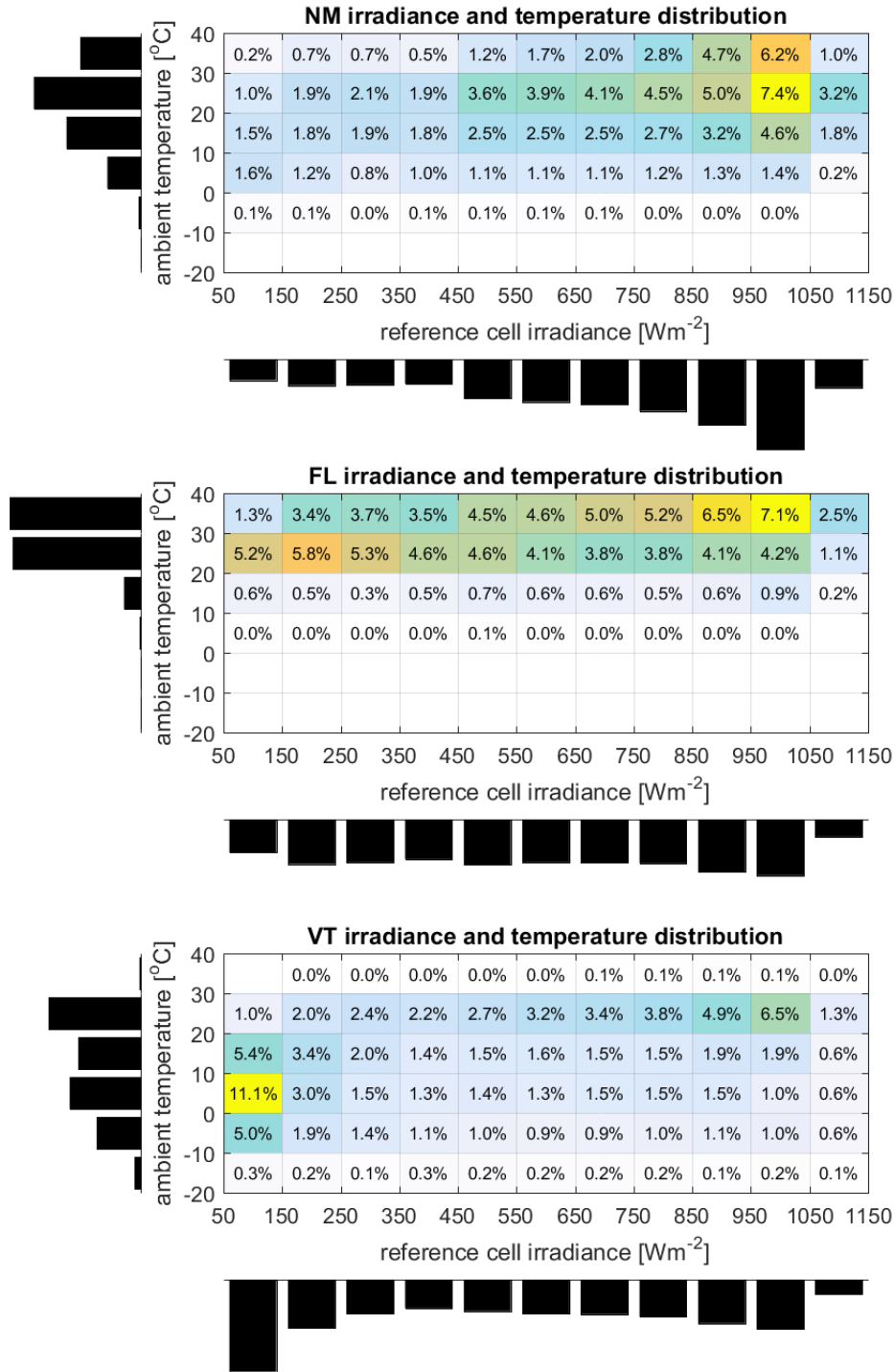


Figure 8: Two-dimensional histograms showing what percent of values passing the solar-time filter fall into each irradiance/ambient temperature bin. For example, of all times passing the solar-time filter in New Mexico, 6.2% of those times are in the bin where irradiance was between 950Wm^{-2} and 1050Wm^{-2} and temperature between 30°C and 40°C . By contrast, only 0.1% are in the same bin for Vermont.

3.2. Cell Temperatures

Sandia collected backside module temperatures for both the baseline and the Stion arrays and then converted the temperature measurements to cell temperatures using the follow equation from the Sandia Array Performance Model [1]:

$$T_c = T_m + \frac{E}{1000 \text{ Wm}^{-2}} \times \Delta T, \quad (1)$$

where T_c is the cell temperature, T_m is the module temperature, E is the reference-cell-measured irradiance, and ΔT is the temperature difference between the cell and the module at 1000 Wm^{-2} . Because the baseline modules are glass/cell/polymer, we use the suggested value of $\Delta T = 1^\circ\text{C}$ [1]. Because the Stion modules are glass/cell/glass, so we use $\Delta T = 3^\circ\text{C}$. With only a 2°C difference, these values will not significantly impact the results shown below, where temperatures range -10°C to 70°C .

The resulting cell temperatures for a module in baseline string 1, and for a module in Stion array 1, string 1, are shown in Figure 9. As an overall trend, cell temperatures increase with increasing ambient temperature, but there is a wide range of cell temperatures at any given ambient temperature due to variations in irradiance.

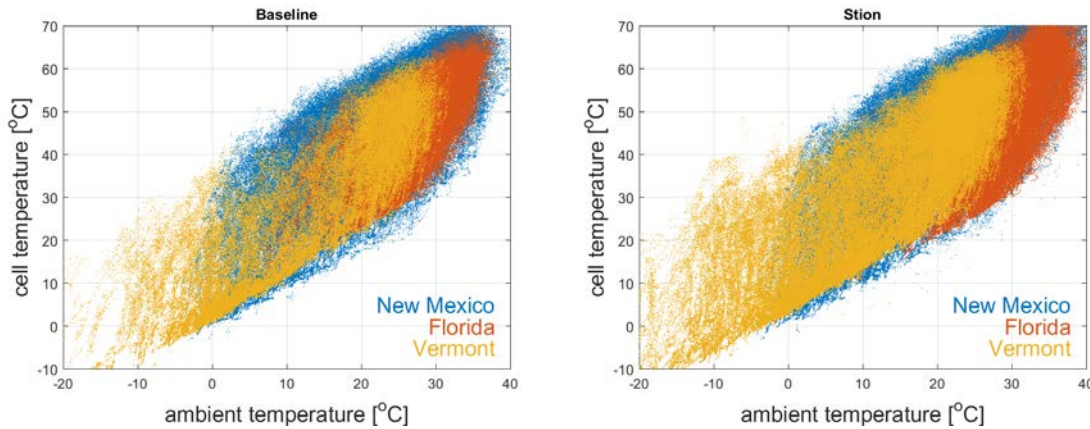


Figure 9: Cell temperatures, which were calculated using the above equation, are plotted here as a function of irradiance. Temperatures are shown for a baseline module in baseline string 1 (left) and a Stion module in Stion array 1, string 1 (right). Data from each RTC location is indicated by a different color.

As shown in Figure 10, Stion cell temperatures were generally hotter than baseline cell temperatures. Although the extent of the temperature difference varied, Stion temperatures typically exceeded baseline temperatures, especially at high temperatures, such as the $40\text{-}55^\circ\text{C}$ range where Stion cell temperatures were $3\text{-}4^\circ\text{C}$ hotter than the baseline. These slightly hotter temperatures may be due to the darker black color and two layers of glass of the Stion modules which hold heat longer than the blue cells and white backsheets of the baseline modules.

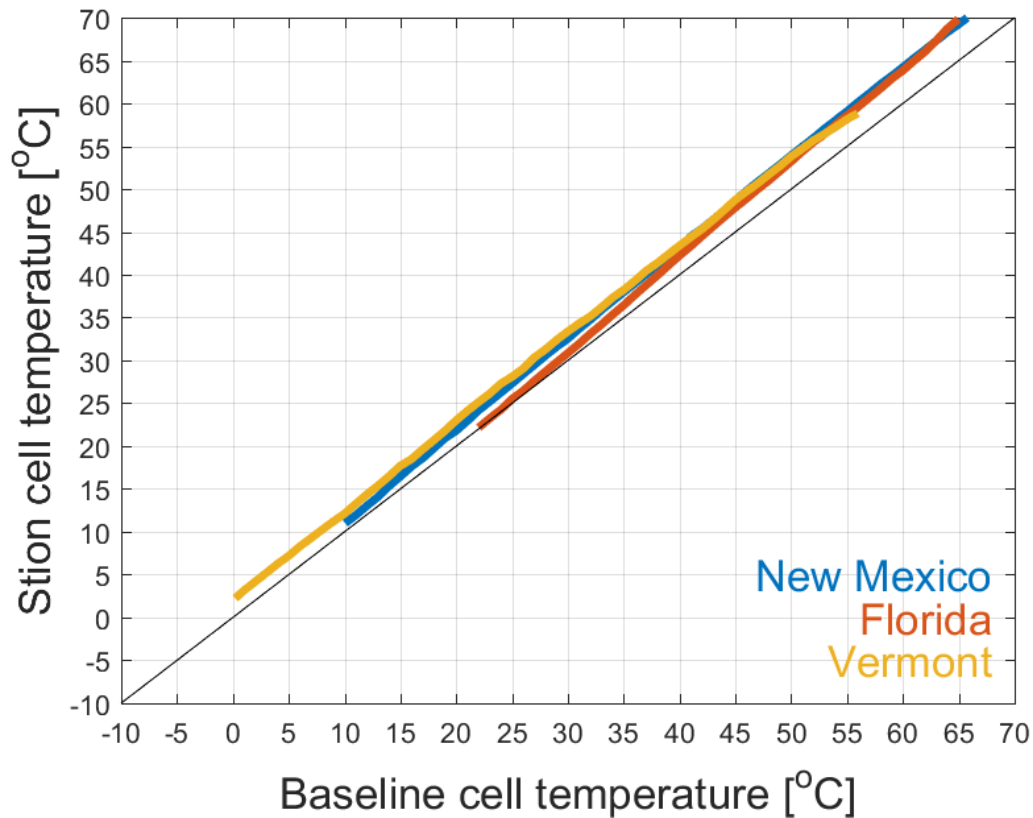


Figure 10: Stion versus baseline cell temperatures. The Stion cell temperatures plotted on the y-axis are median values at 1°C intervals (i.e., the median of all Stion cell temperatures when the baseline cell temperature was within +/- 0.5°C of the value listed on the x-axis).

3.3. Impact of Snow Cover

In Vermont, weather data from the Burlington Airport (less than three miles from the VT RTC) indicates there was a snow event on 141 out of the 708 days considered in this analysis, or roughly 20% of the days analyzed. It is therefore reasonable to conclude that the speed of snowmelt is an important determinant of PV performance in Vermont.

In a few instances, snow appears to melt faster off the Stion modules than the baseline modules. The latter is suggested by Figure 11, where the Stion power output exceeds the baseline power output on the morning of February 12th. Notably, at around noon, the ratio of baseline to Stion power drastically increases, presumably due to snow melting off the baseline modules. This same trend is seen in the picture and plot in Figure 12. However, since the amount of snow on the modules was not explicitly recorded and time-stamped, it is difficult to conclusively determine if snow is consistently melting faster off of the Stion modules; a strategically installed camera could be considered for the Vermont RTC.

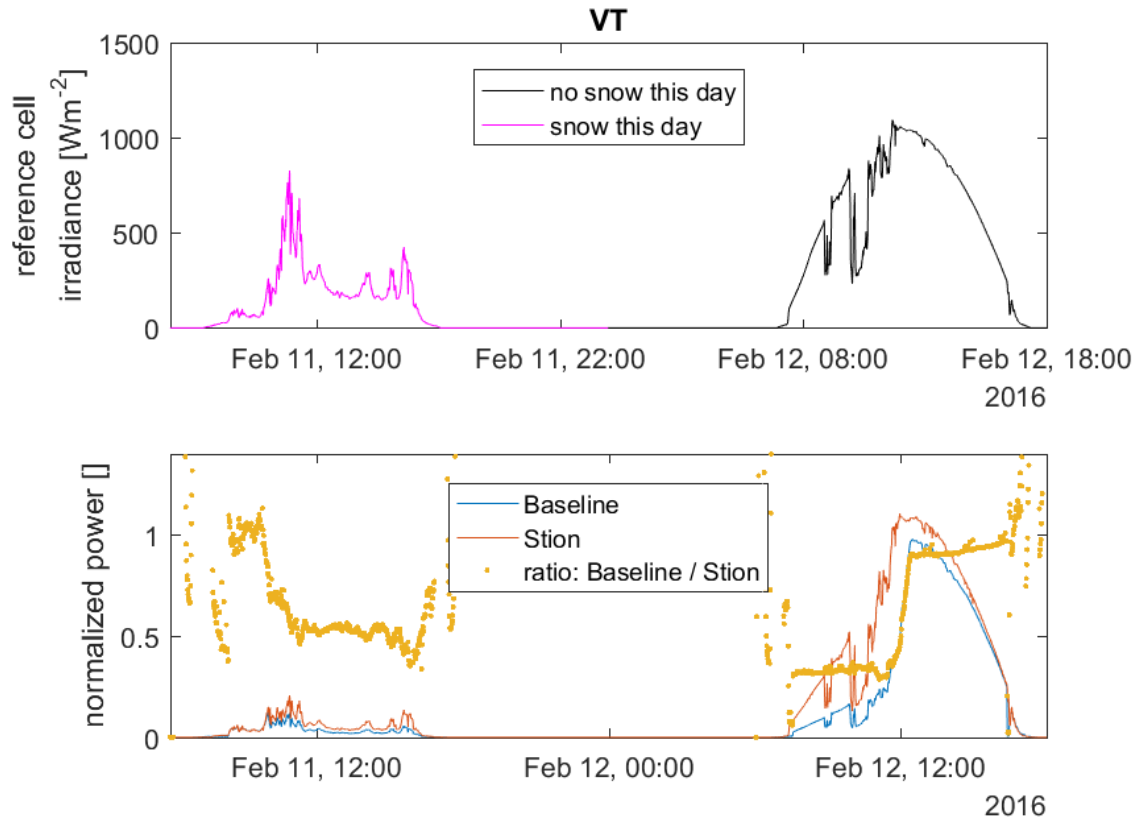


Figure 11: Impact of snow at Vermont RTC. Graphs of reference cell (top) and DC power (bottom) irradiance measurements on a day with snow, followed by a mostly clear day without snow, show the impact of snowmelt.

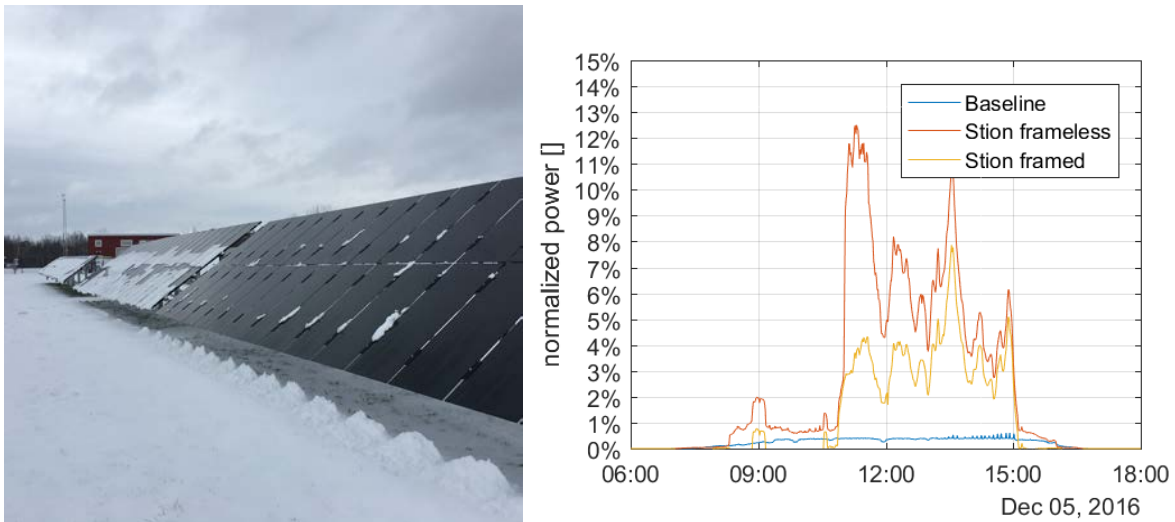


Figure 12: Photo (left) showing the contrast in snow cover between the baseline system (background, far left) and Stion framed arrays (middle) and Stion frameless arrays (foreground) on December 5, 2016. The impact on power output (right) is evident: the Stion systems, with less snow cover, produce more power than the baseline system.

3.4. DC Performance Ratio

The different strings in the baseline and Stion systems at all three locations were in good agreement, and no major errors were noted at any location for either baseline string 1 or Stion array 1 string 1. For that reason, we have chosen to focus on those two strings for our string-level DC performance ratio analysis, believing that the results of the following analysis would not significantly change by using different strings.

In this section, string-level DC performance ratios (PR_{DC}) are calculated as:

$$PR_{DC} = \frac{\text{string } DC_{power} / \text{string } P_{max}}{\frac{\text{POA irradiance}}{1000 \text{ Wm}^{-2}}}, \quad (2)$$

where string P_{max} is the module P_{max} times the number of modules per string (see Table 1). POA irradiance measured from the reference cells were used. DC performance ratio is also referred to as “normalized efficiency” by some researchers [2-3].

We note that PR_{DC} represents a sting-level DC performance ratio. This will vary from module-level performance (such as spec sheet values) in the sense that string-level effects such as mismatch between modules or errors in inverter maximum power point tracking will reduce the string-level PR_{DC} .

3.4.1. Performance Ratio at Constant Irradiance

Figure 13 shows the PR_{DC} of the baseline and the Stion strings as a function of temperature, for relatively constant irradiances around 1000 Wm^{-2} . The plots show a clear decline in PR_{DC} as temperature increases for both module types (i.e., both have negative slopes). Note that the cell temperatures for the Stion modules are slightly hotter, on average, than for the baseline modules, as indicated by the increase in data points at high temperatures for the Stion strings.

But the data also indicates that the baseline modules have lower PR_{DC} , with values of around 0.95 at 25°C cell temperatures or an output of only 95% of rated power at approximately STC conditions. In contrast, the Stion modules appear to have PR_{DC} values above 1 at 25°C cell temperatures, suggesting they are slightly outperforming their rated power.

Overall, the PR_{DC} results are consistent across the three RTC sites. That said, the baseline system in New Mexico demonstrates slightly higher PR_{DC} at the higher temperatures in New Mexico than the baseline system in Florida, but there is only about 5% variation at each temperature. Similarly, Stion values are generally within 5% across the different locations. The cooler temperatures in Vermont are evident by the many points resolved at cell temperatures below 25°C .

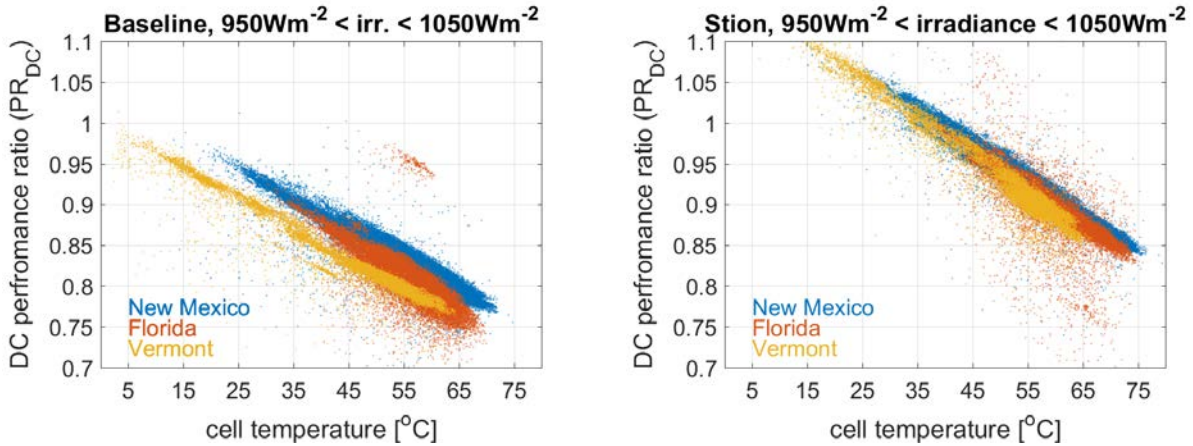


Figure 13: Relative DC performance ratio (y-axis) as a function of cell temperature, filtered to show only times when the irradiance was between 950Wm^{-2} and 1050Wm^{-2} for the baseline (left) and Stion modules (right). Data from each RTC location is indicated by a different color.

3.4.2. Performance Ratio at Constant Temperature

The PR_{DC} at nearly constant temperatures (between 20° and 30°C) are shown in Figure 14. All three locations show consistent results, with the exception of low irradiance ($<100\text{Wm}^{-2}$) for the baseline modules. Overall, the variation of PR_{DC} at each irradiance level can reach about 10%, due to the strong temperature dependence of PR_{DC} , as seen in Figure 13. No large offsets between the different locations are observed.

The baseline modules have nearly constant PR_{DC} as a function of irradiance, especially for irradiances greater than 200Wm^{-2} . In contrast, the PR_{DC} of the Stion modules shows a clear dependence on irradiance, with PR_{DC} increasing in parallel with irradiance.

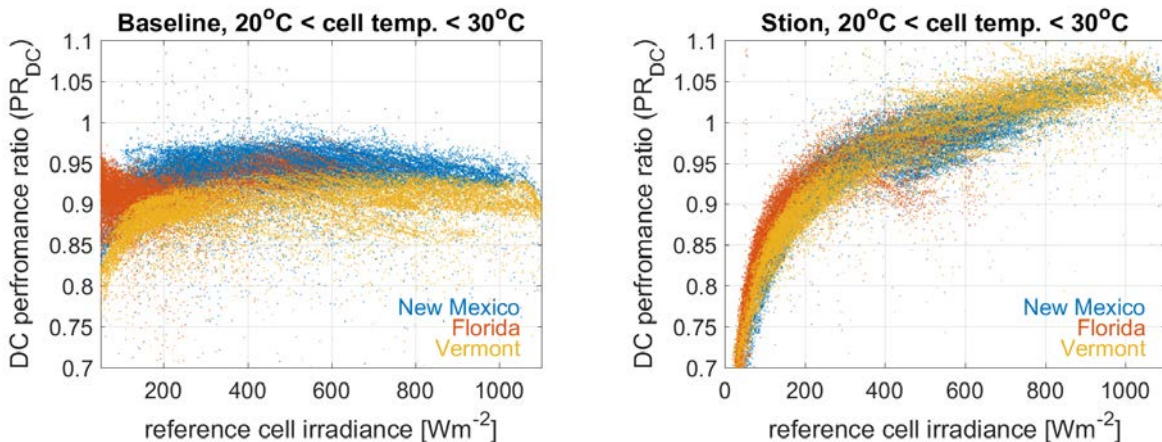


Figure 14: DC performance ratio (y-axis) as a function of reference cell irradiance with cell temperatures between 20°C and 30°C for baseline modules (left) and Stion modules (right) Data from each RTC location is indicated by a different color.

To explore this PR_{DC} dependence on irradiance, we evaluated separately the current and voltage behavior as a function of irradiance. To do this, we found temperature-corrected maximum power point voltage (V_{mp}) and current (I_{mp}) values from the recorded data, following the procedure to determine Sandia Array Performance Model (SAPM) coefficients described in [4]. Our procedure varied fundamentally from the typical method to determine temperature coefficients in that we used in-situ, fixed-tilt, string-level measurements of voltage and current instead of I-V curve measurements from tracker-mounted single modules. Specifically, here we (a) assumed that measured current and voltage values (those described in section 2.2) are the current and voltage at the maximum power point and (b) we derived string-level performance coefficients. Only irradiance values between 990 and 1010 Wm^{-2} were used ensure that the impact of changing irradiance was small.

Temperature-corrected current and voltage values are presented in Figure 15. For easier comparison between baseline and Stion systems, the current and voltage values in Figure 15 are normalized by manufacturer data sheet I_{mp_0} and V_{mp_0} values (8.7A and 31V per module for baseline and 2.34A and 59.8V per module for Stion). Specifically:

$$I_{mp_{Tr,norm}} = \left(\frac{I_{mp}}{1 + \hat{\alpha}_{I_{mp}} \times (T_c - 25^\circ C)} \right) / I_{mp_0}$$

$$V_{mp_{Tr,norm}} = \left(V_{mp} - \beta_{V_{mp}} \times (T_c - 25^\circ C) \right) / V_{mp_0}$$

Also included in Figure 15 are plots showing the temperature corrected PR_{DC} as a function of irradiance:

$$PR_{DC,Tr} = \frac{I_{mp_{Tr,norm}} \times V_{mp_{Tr,norm}}}{\frac{POA \text{ irradiance}}{1000 Wm^{-2}}}$$

The increasing $PR_{DC,Tr}$ as a function of irradiance for the Stion modules appears to be due to increasing voltage with increasing irradiance.

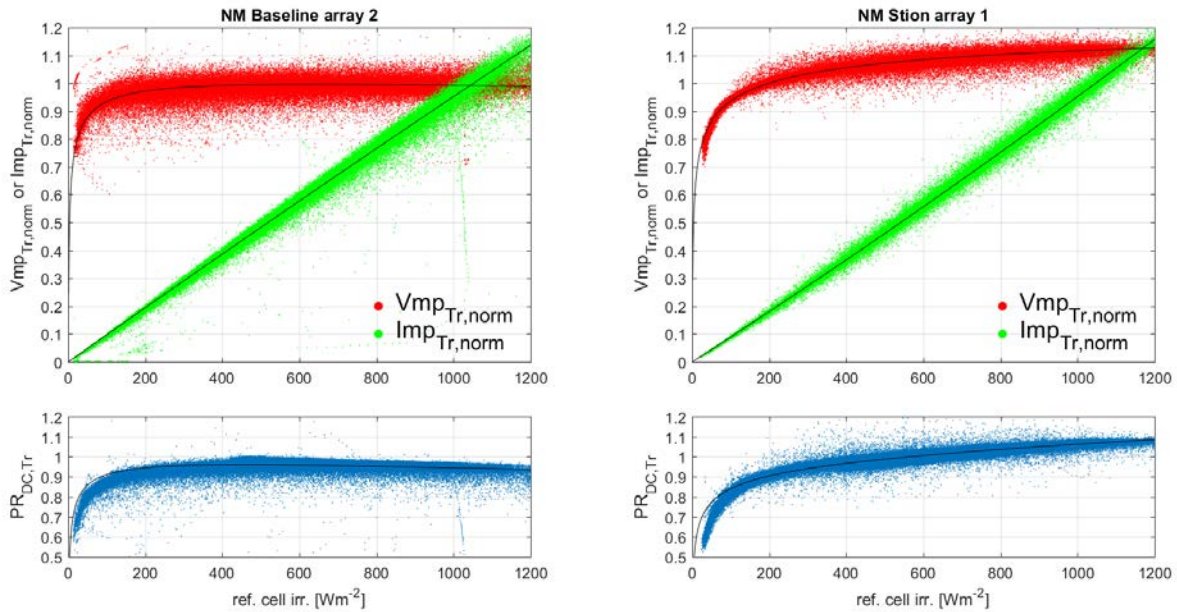


Figure 15: Top Plots: Voltage and current, temperature corrected and normalized by manufacturer data sheet values, plotted as a function of irradiance. Bottom plots: temperature

corrected PR_{DC} as a function of irradiance. Left side plots shows baseline array two and right side plots show the aggregate of Stion arrays 1-4.

The increasing PR_{DC} and voltage as a function of irradiance seen in Figures 14 and 15 is a surprising result: voltage is not expected to have a large irradiance dependence, especially at mid to high (~ 200 to 1000 Wm^{-2}) irradiance levels. We compared the results shown above to SAPM coefficients derived in the traditional sense: from tracker data, collecting module-level I-V curves, which are shown in Figure 16. This tracker data is generally consistent with the results seen above: temperature corrected voltage increases as a function of irradiance for the Stion module, but is relatively constant with changing irradiance for the baseline module.

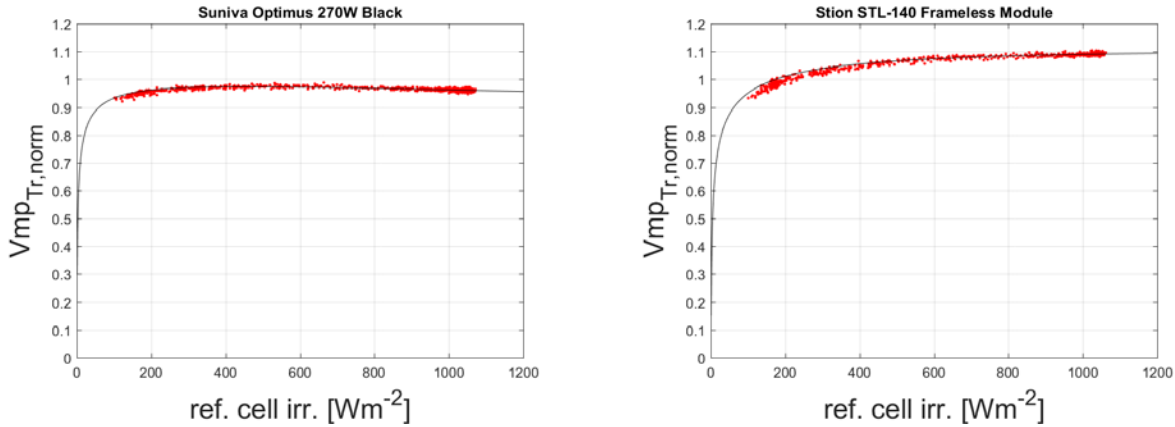


Figure 16: Maximum power point voltage, as measured from a module mounted on a tracker,, temperature corrected and normalized by spec sheet value, plotted as a function of irradiance for (left) a baseline module and (right) a Stion module. The axis range is the same as the top plots of Figure 15 to allow for comparison.

3.4.3. DC Performance Ratio Joint Dependence on Irradiance and Temperature

Figure 17 shows the median PR_{DC} values for each irradiance/temperature bin as two-dimensional color plots. The coupled irradiance and temperature dependence of PR_{DC} can be seen, as can the distribution of irradiance and cell temperatures for each location. For example, cell temperatures in New Mexico commonly range from 0°C to 70°C , while in Florida they range from 20°C to 70°C , and in Vermont from -10°C to 60°C . The highest temperatures ($>60^\circ\text{C}$) are most commonly seen in New Mexico.

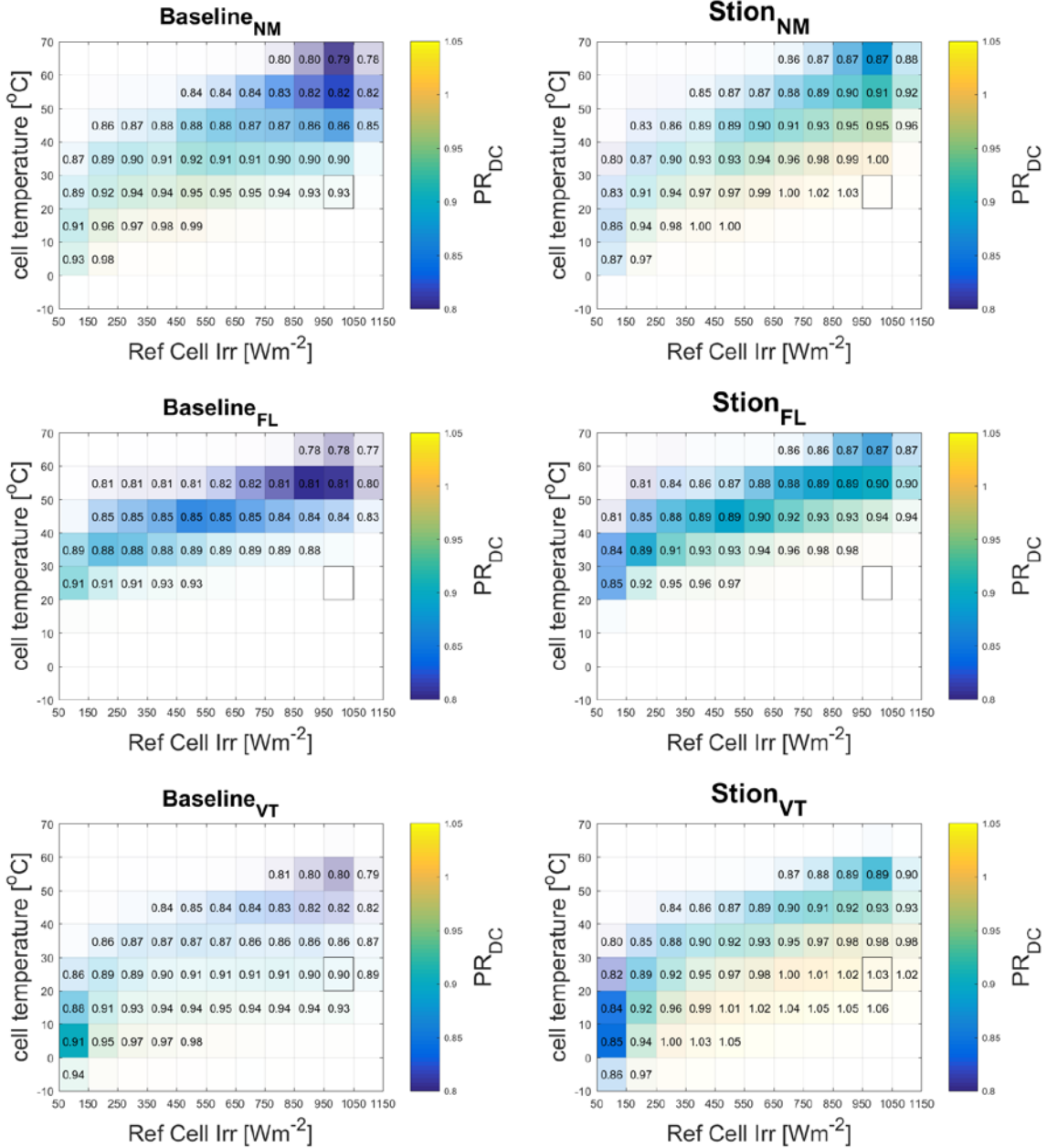


Figure 17: DC performance ratio (colors) as a function of reference-cell irradiance (x-axis) and module temperature (y-axis) bins. Colors (blue to yellow) show PR_{DC} , with blue representing the lower and yellow the higher values. Color intensities (strong vs. faded) indicate the relative number of data points in each bin: stronger colors indicate more data points. The black square indicates the bin containing STC conditions.

3.4.4. Monthly DC Performance Ratio

Here, we average PR_{DC} over month-long periods to show seasonal trends and changes in system performance.

$$\text{monthly } PR_{DC} = \frac{\sum_{\text{month}} \text{string } DC_{power}}{\frac{\sum_{\text{month}} \text{irradiance}}{1000 \text{ Wm}^{-2}} \times \text{string Pmax}}, \quad (3)$$

Monthly PR_{DC} for the New Mexico system (see Figure 18) reveal distinct seasonal trends, with higher PR_{DC} in winter and lower PR_{DC} in summer. Note one anomaly in the data: Stion array 2, string 1, had a module failure in September, 2015, causing string performance to suffer by about 10% compared to the other Stion strings.

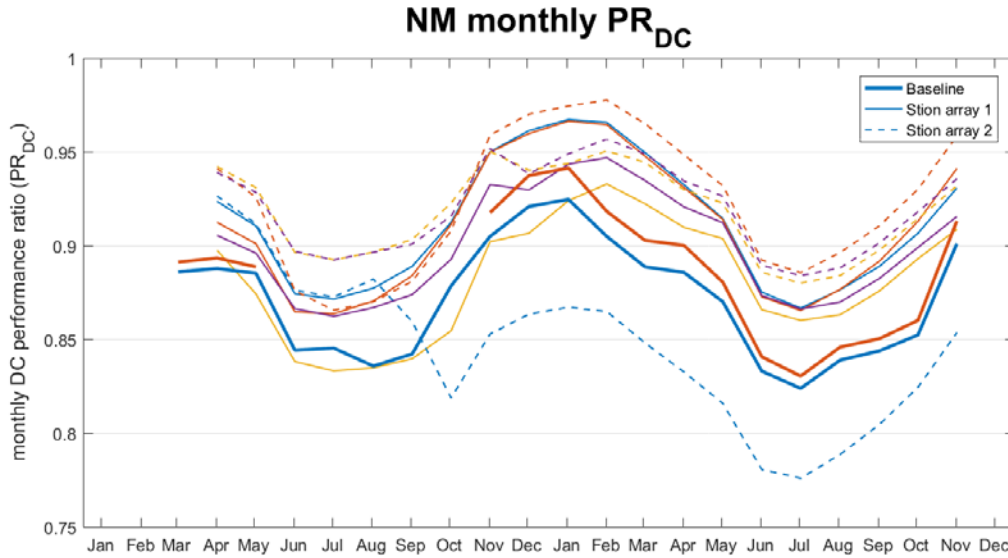


Figure 18: Monthly PR_{DC} in New Mexico for each of the baseline (thick lines) and Stion 1 (thin lines) and Stion 2 (dashed lines) arrays. Colors blue, red, yellow and magenta correspond to strings 1, 2, 3, 4.

Changes in monthly PR_{DC} for the Florida system (see Figure 19) are less pronounced because Florida has less seasonal temperature variation. In Florida, the baseline, string 2, had a module failure in late May 2016, leading to the reduced PR_{DC} that is visible in June, July, and August 2016.

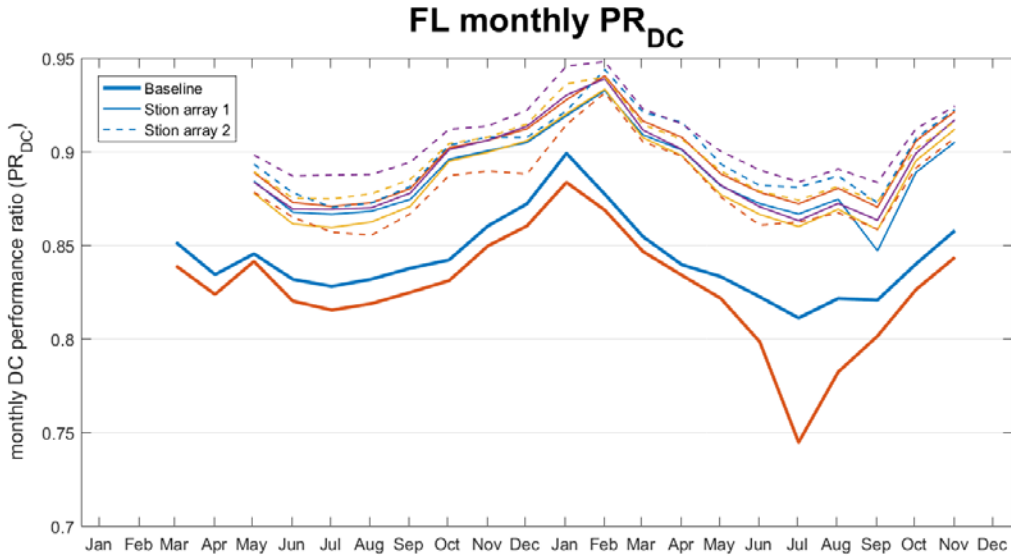


Figure 19: Monthly PR_{DC} in Florida for the baseline (thick lines) and Stion array 1 (thin lines) and Stion array 2 (dashed lines). Colors blue, red, yellow, magenta correspond to strings 1, 2, 3, 4.

Monthly PR_{DC} for the Vermont system (see Figure 20) also reveal the impact of module failure, with multiple module failures in Stion array 2, string 2 (June through October 2015) and in Stion array 2, string 3 (May through September 2016). In addition, the large amount of missing baseline data (Figure 2) makes it difficult to discern trends in the baseline performance.

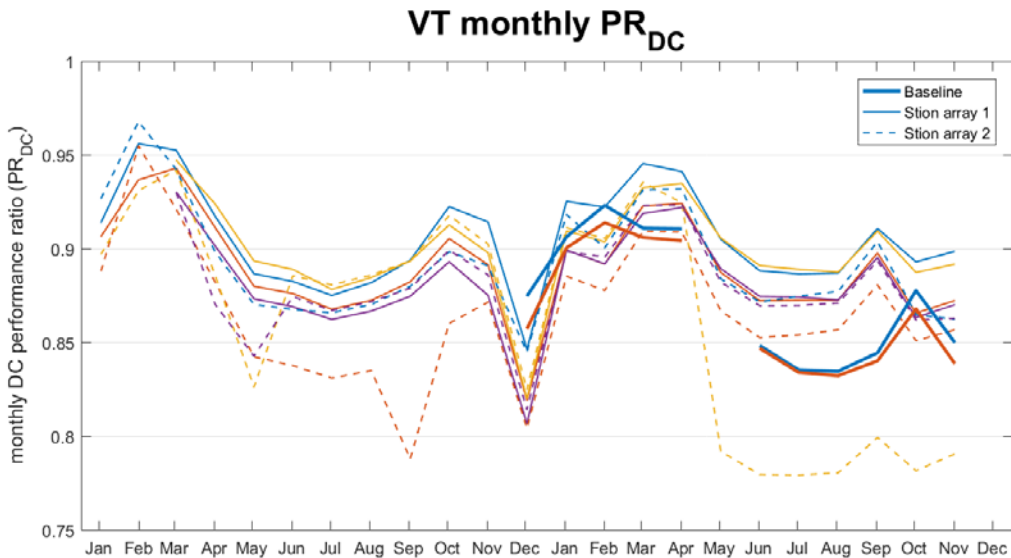


Figure 20: Monthly PR_{DC} in Vermont for the baseline (thick lines) and Stion array 1 (thin lines) and Stion array 2 (dashed lines). Colors blue, red, yellow, magenta correspond to strings 1, 2, 3, 4. Drop in Dec 2015 is likely due to partial snow coverage that was not removed by the current-irradiance filter (>30% difference).

4. CONCLUSIONS

Although module failures occurred at all three RTC sites, temporarily impacting both string performance and data availability, several conclusions can be drawn about the overall performance of the Stion systems at the New Mexico, Florida and Vermont RTCs:

- Stion modules slightly outperform rated power at conditions similar to STC, as indicated by DC performance ratio values slightly above 1 during times when irradiance was close to 1000 Wm^{-2} and temperature was close to 25°C .
- As expected, due to their lower efficiency, Stion cells ran a few degrees hotter than the baseline cells, though both the baseline and Stion cell temperatures were typically hotter than the ambient air temperature.
- The DC performance ratio of Stion modules, like the baseline modules, depends strongly on temperature. Although the Stion modules had higher DC performance ratio values than the baseline modules, both module types seem to have DC performance ratio decrease at a similar rate when temperature increases.
- Stion strings showed an increase in DC performance ratio as irradiance increased, with the steepest slope occurring between zero and 400 Wm^{-2} but DC performance ratio still continues to rise, albeit much more slowly, as irradiance levels reach 1000 Wm^{-2} (In contrast, the baseline string DC performance ratio showed little dependence on irradiance.) It is also noteworthy that the baseline strings do not match the (module-based) Pmax rating at conditions near STC: they are about 6% low.
- Monthly DC performance ratios for both Stion and the baseline show strong seasonal trends in New Mexico, with the highest DC performance ratios in the winter months of January and February and lowest DC performance ratios in July and August. Seasonal trends in Florida, where the temperature range is not as large, are weaker but show a small peak in January and February. Trends in Vermont are difficult to discern due to missing data and irregular performance but are expected to become clearer in the next six to 12 months.
- The Stion modules appear to shed snow faster than the baseline system but this finding needs to be further investigated and quantified.
- Overall, the Stion modules have performed well and there is no evidence of moisture ingress in the Stion STL (frameless) modules.

REFERENCES

- [1] D. L. King, J. A. Kratochvil, and W. E. Boyson, "Photovoltaic array performance model," Sandia National Laboratories SAND2004-3535, 2004.
- [2] B. Herteleer, B. Huyck, F. Catthoor, J. Driesen, and J Cappelle (2017) "Normalised Efficiency of Photovoltaic Systems: Going beyond the Performance Ratio", Solar Energy, Submitted
- [3] "Normalized Efficiency", PV Performance Modeling Collaborative, 2017. [Online]. Available: <https://pvpmc.sandia.gov/modeling-steps/5-ac-system-output/pv-performance-metrics/normalized-efficiency/>. [Accessed: 7- March- 2017].
- [4] B. H. King, C. W. Hansen, D. Riley, C. D. Robinson, and L. Pratt, "Procedure to Determine Coefficients for the Sandia Array Performance Model (SAPM)," *SAND2016-5284*, 2016.

DISTRIBUTION

Stion

Attn: Jon Haeme (1)

jhaeme@stion.com

Attn: Seth Stulgis

sstulgis@stion.com

1	MS0148	Ray Shankles	6012
1	MS0951	Craig Carmignani	6112
1	MS0951	Bruce King	6112
1	MS0951	Dan Riley	6112
1	MS0951	James Stephens	10661
1	MS1033	Shannon Boynton	10661
1	MS1033	Abraham Ellis	6112
1	MS1033	Joshua Stein	6112
1	MS1104	Charles Hanley	6110
1	MS1140	Laurie Burnham	6113
1	MS9052	Matthew Lave	6112
1	MS0899	Technical Library	9536 (electronic copy)



Sandia National Laboratories